Room temperature magnetoelectric properties of type-II InAsSbP quantum dots and nanorings

K. M. Gambaryan' , V. M. Aroutiounian, V. G. Harutyunyan, O. Marquardt, and P. G. Soukiassian

Citation: Appl. Phys. Lett. **100**, 033104 (2012); doi: 10.1063/1.3676437
View online: http://dx.doi.org/10.1063/1.3676437
View Table of Contents: http://aip.scitation.org/toc/apl/100/3
Published by the American Institute of Physics

Room temperature magnetoelectric properties of type-II InAsSbP quantum dots and nanorings

K. M. Gambaryan,[1,a)] V. M. Aroutiounian,[1] V. G. Harutyunyan,[1] O. Marquardt,[2] and P. G. Soukiassian[3]
[1]*Department of Physics of Semiconductors and Microelectronics, Yerevan State University, 1 A. Manoogian, Yerevan 0025, Armenia*
[2]*Tyndall National Institute, Lee Maltings, Dyke Parade, Cork, Ireland*
[3]*Commissariat à l'Energie Atomique et aux Energies Alternatives, Laboratoire SIMA, DSM-IRAMIS-SPCSI, Bât. 462, Saclay, 91191 Gif sur Yvette Cedex, France and Université Paris-Sud, 91405 Orsay Cedex, France*

(Received 8 September 2011; accepted 18 December 2011; published online 17 January 2012)

Quaternary InAsSbP quantum dots (QDs) and quantum rings (QRs) are grown on InAs (100) substrates by liquid phase epitaxy. High resolution scanning electron and atomic force microscopes are used for the characterization. The room temperature optoelectronic and magnetoelectric properties of the InAsSbP type-II QDs and QRs are investigated. For the QD-based structures, specific dips on the capacitance-voltage characteristic are revealed and measured, which are qualitatively explained by the holes thermal and tunnel emissions from the QDs. Specific fractures at room temperature are experimentally found in the magnetic field dependence of an electric sheet resistance for the InAsSbP QRs-based sample. © *2012 American Institute of Physics*. [doi:10.1063/1.3676437]

Semiconductor quantum dots confine electrons and holes in all three directions, and this property is making them very attractive for optoelectronic devices not only for improved laser diodes, but also for single photon sources, quantum computing systems and new generation quantum dot (QD)-photodetectors.[1] Among quantum size objects' fabrication techniques, the self-organized Stranski–Krastanow (S–K) method is an important one by which dislocation-free nanostructures can be produced.[2] The well established liquid phase epitaxy (LPE) growth technique has been improved in order to allow for a better thickness control and reproducibility for thin layer epitaxy despite the high initial growth rate. The modified LPE has been employed to grow quantum well heterostructure lasers,[3] QD and QD/nanopits cooperative structures.[4–7]

In this Letter, we present an example of quasi-ternary InAsSbP QDs and quantum rings (QRs) growth on InAs (100) substrates by modified LPE. The InAsSbP type-II QDs and QRs room temperature optoelectronic and magnetoelectric properties, as well as capacitance-voltage characteristics are investigated.

For the growth of quantum size objects we use a step-cooling version of LPE with a modified slide-boat crucible, where nucleation is performed from a thin (tunable from 200 to 1000 μm in height) liquid phase. As a starting point, we use the quaternary liquid phase composition that corresponds to the $InAs_{0,742}Sb_{0,08}P_{0,178}$ alloy in solid phase, that is conveniently lattice-matched to InAs substrate. The InAs (100) substrates have a diameter of 11 mm and are undoped, with a background electron concentration of $n = 2 \times 10^{16}$ cm^{-3}. To obtain strain-induced nanostructure formation in the S–K mode, we use the liquid phase supersaturated by antimony (for the growth of QDs) and by both antimony and phosphorus (for the nucleation of QRs). The antimony and phosphorus concentrations in liquid phase were chosen to provide a lattice mismatch of up to 2% between the InAs substrate and InAsSbP wetting layer at initial growth temperature of T = 550 °C.

In Fig. 1, the atomic force microscopy (AFM) (Asylum Research MFP-3D) images of the InAsSbP type-II QDs in plain (a) and oblique (b) view, as well as the high-resolution scanning electron microscopy (HR-SEM) (SEM-EDXA–FEI Nova 600-Dual Beam) images (c) of the QRs (d and e—enlarged view) grown by LPE on InAs (100) substrate are presented.

These structures were grown from the quaternary In–As–Sb–P liquid phase of 500 μm in height and contact duration with the substrate of 20 min. At the growth of QRs phosphorus and antimony concentrations in liquid phase were chosen twice as high as those at the growth of QDs. A statistical exploration shows that the QDs average density ranges from 6 to 8×10^9 cm^{-2} with heights and widths from 0.5 nm to 20 nm and 10 nm to 60 nm, respectively. The QRs' average density is equal to (1-3) $\times 10^9$ cm^{-2} with the average height and outlet diameter of 10 nm and 35 nm, respectively. Gauss-like distribution on the dependence of number versus average diameter for both QDs and QRs were observed.

Ring-shaped semiconductor nanostructures have gathered growing attention in recent years.[8] These structures have many interesting electronic properties and confine carriers into ring-like quantum states. QRs also provide a means to study quantum effects involving magnetic flux. Most of the experimental work in this field was performed using mainly molecular beam epitaxy (MBE) technique and, in particular, have been done on the InGaAs/GaAs material system.[9]

For the investigation of electrophysical, optoelectronic and magnetic properties of our nanostructures, we fabricated three device structures in the form of photoconductive cells (PCC). The first (test) sample is made of n-InAs (100) bulk industrial substrate with the parameters described above. The second sample is made of the same substrate, but with

a)Electronic mail: kgambaryan@ysu.am.

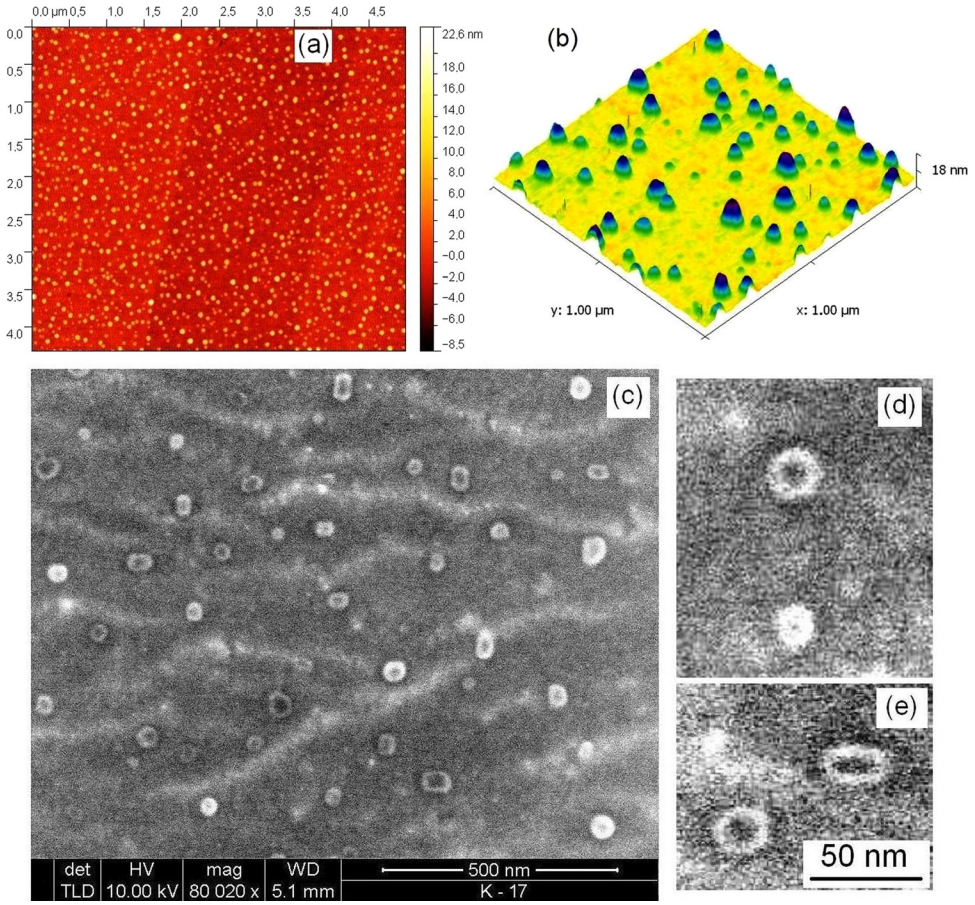

FIG. 1. (Color online) AFM images of the InAsSbP type-II QDs in plain (a) ($S = 5 \times 4.3\ \mu m^2$) and oblique (b) ($S = 1 \times 1\ \mu m^2$) view, as well as HR-SEM images (c) ($S = 1.4 \times 1.4\ \mu m^2$) of the QRs (d and e—enlarged view) grown by LPE on InAs (100) substrate.

type-II InAsSbP QDs (Figs. 1(a) and 1(b)), and the third one with QRs (Figs. 1(c)–1(e)) grown on the substrate surface. The active surface area of these structures is the same and equals 1 mm^2. The topology of the ohmic contacts was chosen to provide needed requirements for the PCCs. Current-voltage (I–V) measurements show, that the electrical sheet resistance of sample 2 is more than one order higher than for sample 1, which can be explained by the charge carrier (light holes) localization inside the QDs. Precise I–V measurements (Keithley-6514 System Electrometer) performed at room temperature also show that for sample 2, a deviation from linearity occurs in the range of 0.52–0.58 V positive applied voltages. In order to definitely state that only the influence and contribution of QDs are responsible for that deviation, we also measured the capacitance-voltage (C–V) characteristics of the prepared samples using High precision capacitance spectrometry (QuadTech-1920 precision LCR meter). The results of room temperature C–V measurements for the first and the second samples performed at $f = 10^6$ Hz frequency are presented in Fig. 2(a).

As can be seen two specific dips on the QDs-based sample's C–V curve are observed at 0.28 and 0.54 V, which do not appear on the first sample's curve. We also suspect that additional hidden dips exist at low voltages, which can be revealed in low temperature measurements. The results of accurate measurements in the range of 0.2–0.4 V and 0.5–0.62 V with the polynomial fitting curves are presented in Figs. 2(b) and 2(c), respectively. We assume that revealed dips are attributed to the ground and exited energy levels for holes in a sub-bandgap created by the QDs. The presence of an electric field tilts the band structure, which may lead to three mechanisms of emission enhancement: (*i*) the Poole–Frenkel effect,[10] when the carrier is still emitted by thermal activation over the top of a potential barrier, which is lowered by the presence of an electric field, (*ii*) pure tunneling, and (*iii*) phonon-assisted tunneling, where the carrier absorbs energy from the lattice and then tunnels through the barrier at higher energy. In our type-II InAsSbP QDs system the apparent difference in the emission mechanisms for heavy and light holes is attributed to the different effective masses, since the tunneling probability is inversely proportional to the effective mass.[10]

For InAs, the heavy hole effective mass is typically by a factor of 10 larger than the light hole (and electron) effective mass. However, light hole and electron effective masses are approximately the same and equal to $\sim 0.028\, m_0$. In our case we assume that light holes from the ground state are emitted by direct tunneling through the triangular barrier, and/or from the ground state are thermally activated into excited states and subsequently emitted by thermal and tunnel emission, whereas heavy holes are emitted by pure thermal activation from the ground state into the InAs substrate's valence band. But this is not always the case. Because of the symmetry breaking and 3D confinement, what we refer to as heavy hole states can also include a small amount of light hole character, and this light hole character can then contribute to the tunneling. However, based on C–V measurements, we experimentally calculated the activation energy $(h_1 - h_0)$ in our system which is equal to ~ 0.26 eV at room temperature. The similar approach has been applied in Ref. 11,

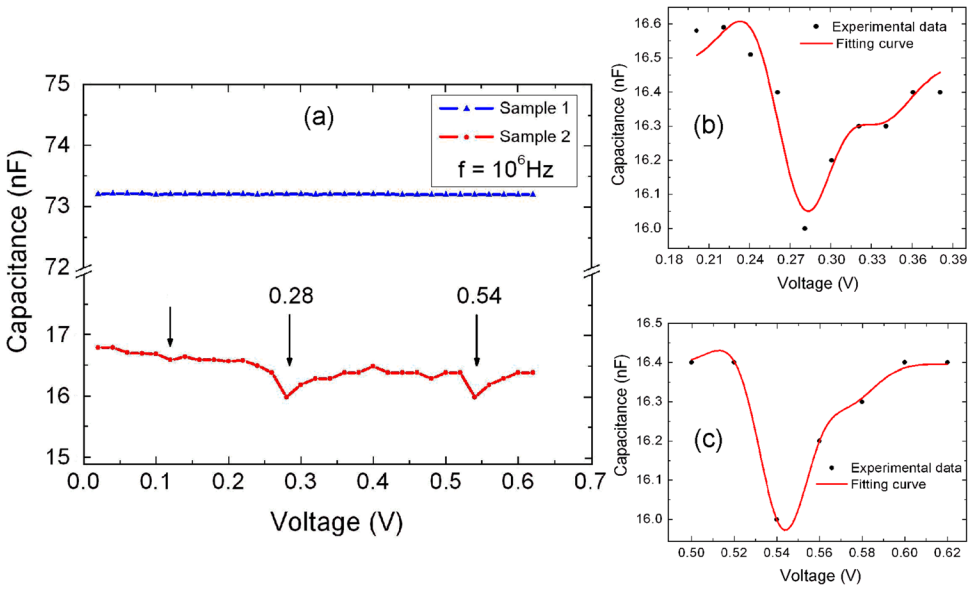

FIG. 2. (Color online) (a)—Room temperature high-precision C–V characteristics of sample 1 (blue triangles) and sample 2 (red circles); (b) and (c)—an enlarged view of dips with the polynomial fitting curves.

where the electronic energy levels of InAs QDs were measured with respect to the GaAs conduction band edge by employing capacitance–voltage spectroscopy.

Type-II QDs and QRs (samples 2 and 3 in our case) are distinctly different from single or multiple stacked type-I QDs and the charge carrier distribution and geometry are more complicated. This geometry makes them particularly interesting for studies in magnetic fields, because for both cases this geometry defines a ring-like trajectory for electrons (or holes), ensuring that for instance in our type-II InAsSbP QDs the electron wave function is delocalized, as we have confirmed in previous calculations based on an eight-band **k**·**p**-simulation.[4] Here, the free particle is the electron rather than the hole, which has a smaller effective mass. A strong band gap bowing in InAsSb induces a shallow conduction band minimum in InAsSb. However, strain effects in the systems studied in Ref. 4 due to the lattice mismatch to the surrounding InAs matrix compensate for this minimum in the conduction band offset and prevent an electron localization in InAsSb QDs. The magnetic flux leads to a periodic change in the quantum mechanical properties of the charge carrier system in QR and encircling the type-II QD. These oscillations are periodic in the applied magnetic field and are known as Aharonov–Bohm (AB) oscillations that have no classical analog.[12] The experimentally observed AB-oscillations of the excitonic energy and the photoluminescence intensity dependence on the magnetic field have been reported in particular for type-II InP/GaAs and ZnTe/ZnSe QDs,[13,14] as well as oscillations of the magnetic moment per electron on self-assembled InAs/GaAs QRs.[15]

We investigated the magnetic field dependence of the electric sheet resistance (magnetoresistance) for our samples at the Faraday (perpendicular to the substrate surface—*Z*) and Voigt (parallel to the substrate surface—*X* and *Y*, at $X \perp Y$) geometries. A magnetic field of up to 1.6 T was applied and measurements were performed at room temperature. The classical behavior of the dependence of the electric sheet resistance versus the magnetic field was measured and observed for the first test sample (Fig. 3(a)). Otherwise, for the QRs-based sample 3, specific fractures (probably due to the AB effect) on the magnetoresistivity curve are revealed and detected (Fig. 3(b)). Fig. 3 also reveals that the values of the third sample's sheet resistance are higher up to one order of magnitude as compared to the reference sample 1. Finally note that investigated samples prepared in the form of photoconductive cells can be directly used as mid-infrared photodetectors, as well as in many other very important mid-infrared applications.

Thus, we have reported an example of quaternary InAsSbP QD and QR growth on InAs (100) substrates by modified LPE. The room temperature magnetoelectric properties of the prepared samples with (and without) type-II

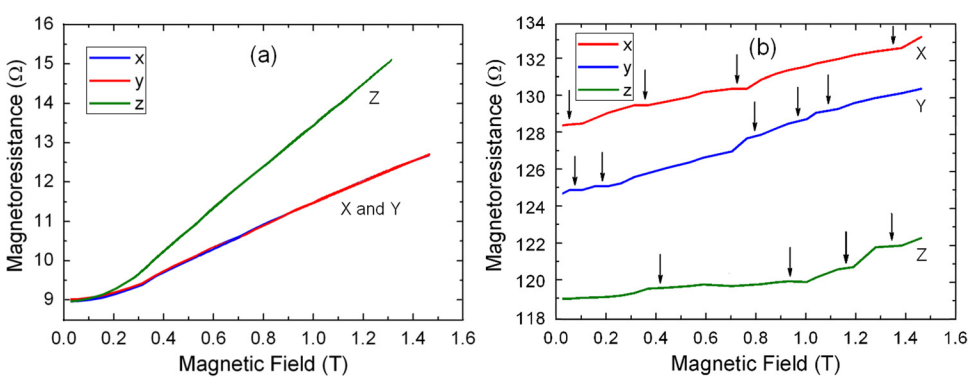

FIG. 3. (Color online) Sheet resistance (magnetoresistance) versus magnetic field at Faraday (perpendicular to the substrate surface—*Z*) and Voigt (parallel to the substrate surface—*X* and *Y*, at $X \perp Y$) geometries of sample 1—(a) and sample 3—(b).

InAsSbP QDs and QRs have been investigated. Specific dips on the C–V curves are detected and qualitatively explained, as well as fractures that were found at room temperature in the magnetic field dependence of the electric sheet resistance for type-II InAsSbP QRs-based sample. Our study opens up interesting fundamental and applied prospects including the underlying physics and technology, understanding the influence of QDs and QRs on InAs-based devices' properties and requires more research effort from both experiment and theory.

This study was performed in the frame of German Academic Exchange Service Research Grant awarded to K. M. Gambaryan at 2010, and in part by a Research Grant from the Armenian National Science and Education Fund based in New York, USA (2011). The authors wish to thank Prof. Dr. Eoin O'Reilly and Prof. Dr. Vladimir Fomin for fruitful discussion, interest to this work and valuable support.

[1]D. Bimberg, M. Grundmann, and N. N. Ledentsov, *Quantum Dot Heterostructures* (Wiley, New York, 1998).
[2]I. Stranski and L. Krastanow, Math.-Naturwiss. **146**, 797 (1938).
[3]N. K. Dutta, R. Yen, R. L. Brown, T. M. Shen, N. A. Olsson, and D. C. Craft, Appl. Phys. Lett. **46**, 19 (1985).
[4]O. Marquardt, T. Hickel, J. Neugebauer, K. M. Gambaryan, V. M. Aroutiounian, J. Appl. Phys. **110**, 043708 (2011).
[5]K. M. Gambaryan, Nanoscale Res. Lett. **5**, 587 (2010).
[6]K. M. Gambaryan, V. M. Aroutiounian, T. Boeck, M. Schulze, and P. G. Soukiassian, J. Physics D: Appl. Phys. (FTC) **41**, 162004 (2008).
[7]K. D. Moiseev, Ya. A. Parkhomenko, A. V. Ankudinov, E. V. Gushchina, M. P. Mikhailova, A. N. Titkov, and Yu. P. Yakovlev, Tech. Phys. Lett. **33**, 295 (2007).
[8]V. M. Fomin and L. F. Chibotaru, J. Nanoelectron. Optoelectron. **4**, 3 (2009).
[9]J.-H. Dai, J.-H. Lee, and S.-C. Lee, IEEE Photon. Technol. Lett. **20**, 165 (2008).
[10]A. D. Yoffe, Adv. Phys. **50**, 1 (2001).
[11]D. Granados and J. M. Garcia, Nanotechnology **16**, S282 (2005).
[12]Y. Aharonov and D. Bohm, Phys. Rev. **115**, 485 (1959).
[13]I. L. Kuskovsky, W. MacDonald, A. O. Govorov, L. Mourokh, X. Wei, M. C. Tamargo, M. Tadic, and F. M. Peeters, Phys. Rev. B **76**, 035342 (2007).
[14]E. Ribeiro, A. O. Govorov, J. W. Carvalho, and G. Medeiros-Ribeiro, Phys. Rev. Lett. **92**, 126402 (2004).
[15]N. A. J. M. Kleemans, I. M. A. Bominaar-Silkens, V. M. Fomin, V. N. Gladilin, D. Granados, A. G. Taboada, J. M. Garcia, P. Offermans, U. Zeitler, P. C. M. Christianen, J. C. Maan, J. T. Devreese, and P. M. Koenraad, Phys. Rev. Lett. **99**, 146808 (2007).